

We are IntechOpen, the world's leading publisher of Open Access books Built by scientists, for scientists

6,900

Open access books available

186,000

International authors and editors

200M

Downloads

Our authors are among the

154

Countries delivered to

TOP 1%

most cited scientists

12.2%

Contributors from top 500 universities



WEB OF SCIENCE™

Selection of our books indexed in the Book Citation Index
in Web of Science™ Core Collection (BKCI)

Interested in publishing with us?
Contact book.department@intechopen.com

Numbers displayed above are based on latest data collected.
For more information visit www.intechopen.com



Role of Intermetallics in Lead-Free Alloys

Dattaguru Ananthapadmanaban and Arun Vasantha Geethan

Abstract

Intermetallics are intermediate compounds formed between two metals. They are usually brittle. The presence of intermetallics leads to deterioration in mechanical properties. This chapter reviews the intermetallic compounds formed during the manufacture of lead-free alloys. Intermetallic compounds formed in ordinary lead-based alloys are also discussed. The role of rare earth, especially indium and lanthanum, additions on intermetallic formation is examined. Microstructures of intermetallics are analysed. Hardness values of lead-free alloys are compared with emphasis on type and nature of intermetallics. SEM photographs of lead-free solders are discussed with regard to type of fracture, and the role of intermetallics in nature of fracture is examined. Lastly, the general mechanisms of formation of intermetallics are touched upon, and these mechanisms are extended to intermetallic formation in lead-free alloys.

Keywords: lanthanum based alloy, indium based alloy, hardness, characterization

1. Introduction

Intermetallic is a type of metallic compound that exhibits definite stoichiometric ratio of atoms. It also has a definite crystal structure. Their role is twofold. In small quantities, they can strengthen the soldering joint. However, when the amount of intermetallics increases, they may render the joint brittle. For example, La_3Sn intermetallics are known to be present in lanthanum-based lead-free alloys. These are known to increase the hardness of the alloys. Ag_3Sn , Cu_3Sn and Cu_6Sn are some known intermetallics in tin-, copper- and silver-based lead-free alloys. Mostly, the interaction of these intermetallics with the substrates has to be studied in detail in order to determine the exact effect on the solder properties. The growth of these intermetallics with time is determined by solid-state diffusion rules and varies from system to system.

2. Intermetallics in lead-based and lead-free solders

Way back in 1972, Lois Zackreysak has reported intermetallics in lead-free alloys. Tin-based lead-free alloys showed the presence of Sn—Cu intermetallic when soldered on a copper-based substrate. It was found that throughout the early stages of the growth process, the Cu_3Sn and the Cu_6Sn_5 thicknesses are approximately equal. As tin is depleted from the solder matrix, Cu_6Sn_5 growth slows down,

while the Cu_3Sn continues to grow at the expense of the tin-rich intermetallic. The presence of insoluble alloying elements affects the intermetallic growth rate to a minor degree. The general theory for the diffusion-controlled growth of plates appeared to be applicable to this metallic system [1].

Just after soldering, Cu_6Sn_5 formed between the solder and copper pad. It should be noted that in most of the soldering joints, there are generally three layers formed. The three layers are substrate, intermetallic and solder. The intermetallic layers are sandwiched between the two substrate layers. In the study mentioned above, microwave energy has been used for soldering [2].

3. Growth kinetics

A study of growth kinetics of any solidification process will be useful to predict the type of microstructure formed and the morphology of the microstructures. Generally, as the alloys solidify under normal cooling conditions, we can expect a dendritic solidification morphology, just like in castings.

During soldering of lead-free alloys, the Cu_6Sn_5 intermetallic sublayer is clearly visible, and the Cu_3Sn sublayer is noticeable only for the sample annealed at 150°C [1].

Comparison of the 63Sn—37Pb joints and the lead-free joints shows that the initial thickness of the intermetallic layer is not significantly impacted by the higher temperature used during the lead-free assembly process. All the values are in a range of 1.6–2.3 microns [3].

The growth of these intermetallic layers can be modelled using parabolic growth kinetics [4]:

$$w = w_0 + D\sqrt{t} \quad (1)$$

where w = thickness of the intermetallic layer, w_0 = initial thickness of the layer, D = diffusion coefficient and t is the time of annealing.

Arrhenius type of growth kinetics is seen.

Li et al. have studied the growth kinetics of Sn-based lead-free solders on copper substrate. The results show that IMC layer is formed at solder-Cu substrate interface within a short time. It was found that Fick's law was not followed. Fick's law states that the mean total thickness increases linearly with the square root of the time. In most of the systems during solidification processing, welding and other manufacturing processes tend to follow Fick's law under equilibrium or near equilibrium conditions. In the case of soldering, cooling is very fast, especially when copper is used as substrate. It deviates from Fick's law at the early stage of the growth process and then approaches the parabolic law [5].

The growth behaviour of intermetallic compounds (IMCs) at the liquid-solid interfaces in Cu/Sn/Cu interconnects during reflow at temperatures in the range of 200 – 300°C on a hot plate, which was investigated by Zhao et al. The interfacial IMCs showed clearly asymmetrical growth during reflow. The growth of Cu_6Sn_5 IMC at the cold end was significantly enhanced while that of Cu_3Sn IMC was hindered especially at the hot end. It was found that the temperature gradient had caused the mass migration of Cu atoms from the hot end towards the cold end, resulting in sufficient Cu atomic flux for interfacial reaction at the cold end while inadequate Cu atomic flux at the hot end. The growth mechanism was considered as reaction/thermomigration-controlled at the cold end and grain boundary diffusion/thermomigration-controlled at the hot end [6].

Guo et al. [7] found that the interfacial Cu_6Sn_5 was much thicker at the cold end, whereas the consumption of Cu was much faster at the hot end in Cu/Sn—2.5Ag/

Cu solder joints during reflow at 260°C on a hot plate, due to the rapid migration of Cu atoms under a simulated temperature gradient of 51°C/cm. Qu et al. [1, 8] in situ studied the soldering interfacial reactions under a temperature gradient of 82.2°C/cm at 350°C using synchrotron radiation real-time imaging technology, and asymmetrical growth and morphology of interfacial IMCs between the cold and hot ends were clearly observed.

4. Hardness results

Hardness, especially microhardness is a very simple engineering measurement that gives information about the material being tested. In the case of volume of measurement being small as is the case of solders, then microhardness measurements are done from the periphery to the centre along any diagonal. In the case of solders, hardness values are an indication of whether intermetallic phases are present or not. For example, if the hardness of a material of a particular composition is higher than the normal solder alloy of the same composition, there is a possibility of intermetallic formation. Microstructural analysis should also be used to confirm the presence of intermetallics.

These hardness results are taken from the author's research work on lead-free alloys. All the values quoted here are experimental values obtained by the author and his team of coresearchers, and they have been published recently [9, 10].

4.1 Indium-based Sn—Zn alloys

All hardness values described in this section are taken along two perpendicular diagonals of a square-shaped specimen. Results are shown in (Table 1).

Sn—37Pb solders normally used for soldering have a hardness of 12 H_V [11]. So, on an average, both the new alloys have hardness higher than the traditionally used lead-based soldering alloys.

Hardness values are shown below in Tables 2 and 3.

Small changes in Zn and Al do not change the hardness much, and literature has shown that even small additions of lanthanum affect the hardness. So, it can be assumed with reasonable certainty that the hardness changes are due to changes in lanthanum content. Small additions of indium have been shown to improve the microhardness and also produce considerable changes in the microstructure [12]. Small amounts of indium addition have been found to refine grain size and improve hardness [13, 14].

Specimen	Hardness, H _V 0.2					Average
Sn—7Zn—3Al—3In	18.4	19.9	19.1	18.8	19.3	19.1
Sn—6Zn—2Al—2.5In	18.6	17.7	18.1	18.3	17.9	18.1

Table 1.
 Results of hardness testing.

Specimen 88Sn—7Zn—2Al—2.5In	Hardness, H _V 0.2				
Diagonal 1	22.42	22.46	24.32	19.92	20.53
Diagonal 2	22.42	19.19	25.21	16.89	19.5

Table 2.
 Hardness value of specimen 88Sn—7Zn—2Al—2.5In.

4.2 Lanthanum-based lead-free alloys

Two solders are analysed for their hardness. Both are lanthanum-based alloys with similar composition. Results are given in **Tables 4** and **5**.

The average hardness for sample 1 is **17.8 HV**.

The average hardness for sample 2 is **18.4 HV**.

Muhammed Aamir et al. [15] investigated that the inclusion of 0.4 wt.% of La in to Sn—Ag—Cu (SAC) solder system results in intermetallic growth. Intermetallics are hard in nature. Hence, our findings are in line with reported work, which indicates increase in hardness on addition of lanthanum.

4.3 Sn—Cu lead-free alloys

Referring **Table 6** above silver and manganese content are more in sample 1. Manganese is known to increase hardness. This could be the reason for higher hardness in sample 1. Since hardness of sample 1 is higher than sample 2, this could indicate the presence of more intermetallics in sample 1. With the addition of La, the microhardness of β -Sn and eutectic area was enhanced from 13.8 to 16.4 Hv and from 16.8 to 18.8 Hv, respectively [16]. Cu_6Sn_5 , Ag_3Sn and MnSn_2 are present in dendritic Sn-rich solid solution (β Sn). These intermetallics are found in both samples as seen in the microstructures of the samples. However, % age of intermetallics in each of the samples may be different. Average hardness of the second sample is considerably lower than the first one. This indicates that the presence of intermetallics is lesser in the second sample. More detailed analysis using XRD is required to

Specimen 88Sn—7.5Zn—2.5Al—2In	Hardness, $H_V 0.2$				
Diagonal 1	17.5	20.9	22.42	22.52	21.9
Diagonal 2	18.6	21.6	21.6	22.41	22.2

Table 3.

Hardness value of specimen 88Sn—7.5Zn—2.5Al—2In.

S.No	Diagonal 1 (μm)	Diagonal 2 (μm)	Microhardness value (HV 0.5) average
1	17.8	17.0	17.4
2	17.45	18.45	17.9
3	20.1	20.5	20.3
4	17.5	15.5	16.2
5	17.8	16.8	17.4

Table 4.

Microhardness value for sample 1 of composition 1 Sn-87.5% Zn-7.5% Bi-4% La-1%.

Diagonal 1 (μm)	Diagonal 2 (μm)	Microhardness value (HV 0.5)
16.5	16.5	16.5
17.3	18.1	17.7
18.6	22.6	20.2
19.5	19.0	19.3
17.6	19.6	18.2

Table 5.

Microhardness value for sample 2 of composition 2 Sn-87% Zn-7% Bi-4.5% La-1.5%.

S No	1	2	3	4	5	6	Avg
Sample 1	26.7	26.4	28.4	32.5	28.5	30.4	28.8
Sample 2	18.1	19.0	17.8	18.3	17.8	15.4	17.7

Table 6.
 Hardness values for the two alloys.

Diagonal 1 (μm)	Diagonal 1 (μm)	Microhardness value (HV 0.5)
22.42	22.42	19.3
22.46	19.19	16.7
24.32	25.21	18.2
19.92	16.89	17.4
22.32	19.05	20.4

Table 7.
 Microhardness value for sample 1.

Diagonal 1 (μm)	Diagonal 1 (μm)	Microhardness value (HV 0.5)
17.5	18.6	16.8
20.9	21.6	17.3
22.42	21.6	20.5
22.52	22.41	19.1
23.44	24.03	17.2

Table 8.
 Microhardness value for sample 2.

come to a final conclusion. Zhang et al. showed that addition of 0.05% rare earth Yb suppressed the growth of intermetallics and the morphology of Cu_6Sn_5 layer can be changed to a relatively flat morphology (Table 6) [17].

4.4 Sn—Zn-lanthanum lead-free alloys

Two samples with slight compositional differences have been analysed, and the results were presented in Tables 7 and 8.

Sample 1 has a composition of Sn-87.5% Zn-7.5% Bi-4% La-1%.

The average hardness for sample 1 is 18.4 HV.

Sample 2 has a composition of Sn-87% Zn-7% Bi-4.5% La-1.5%.

The average hardness for sample 2 is 18.2 HV.

For Sn—8Zn—3Bi, with increasing temperature, the amount of hard Bi segregation increases which is the main cause of the rise in hardness.

Microstructural analysis done in a recent research work by the authors has been analysed.

5. Microstructural and EDAX analysis of Sn—Zn—Al-In alloys

5.1 Analysis of low Al-low indium alloys

Results of experimental work on 88Sn—7.5Zn—2.5Al—2In and 88Sn—7Zn—2Al—2.5 in lead-free soldering alloys are presented below.

Microstructures taken at different locations in the prepared solders showed variations, and the detailed analysis of the microstructures is given below.

Figure 1 shows the microstructure, and **Figure 2** shows the corresponding EDAX line spectrum. The weight % of sigma phase is 0.6%, when we consider the aluminium peak and 1.55% in the zinc peak. The indium cluster is seen in the middle and this showed 0.23% sigma phase. Sigma phase is a hard, brittle phase and generally not desirable. The presence of indium seems to have decreased the amount of sigma phase.

Indium peaks are not seen in **Figures 3** and **4**, when EDAX image is considered, and sigma phase is around 0.93% in both the Zn peak (first from the left) and the aluminium peak (second from the left). Sigma phase % age is more in this case compared to the previous microstructure (**Figures 5** and **6**).

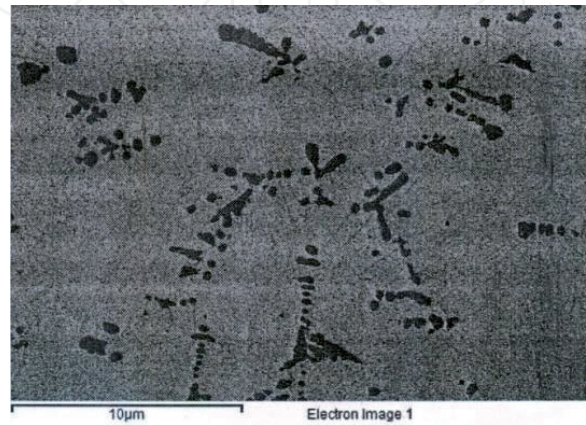


Figure 1.
Spectrum 1 electron image.

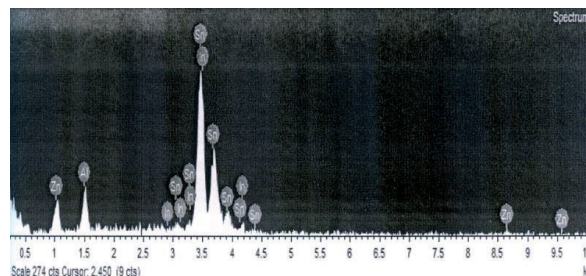


Figure 2.
Spectrum 1 EDAX graph.

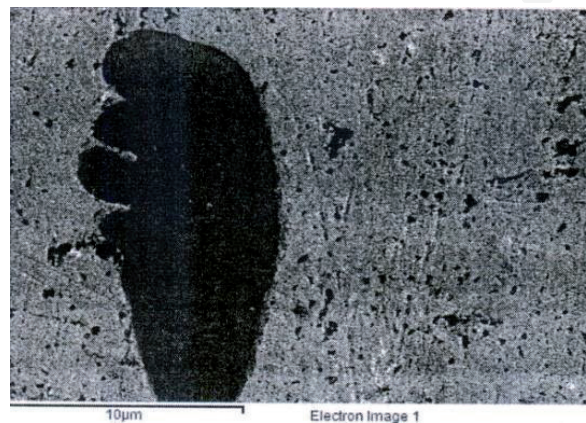


Figure 3.
Spectrum 2 electron image.

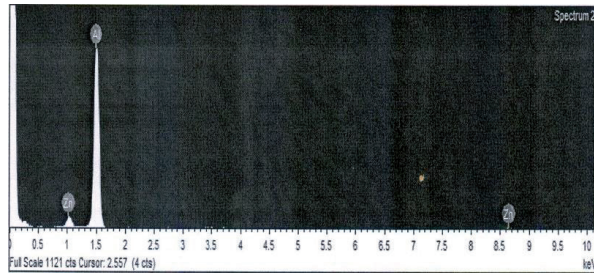


Figure 4.
Spectrum 2 EDAX graph.

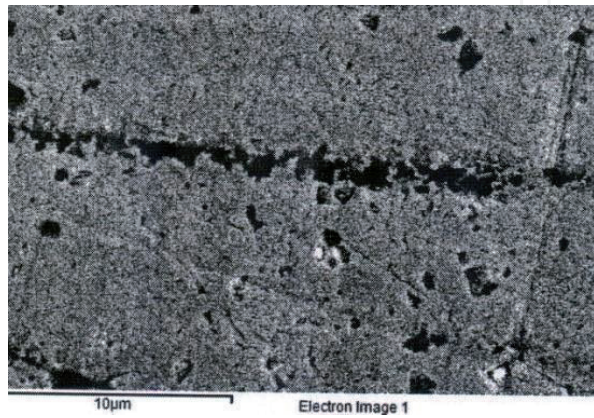


Figure 5.
Spectrum 3 electron image.

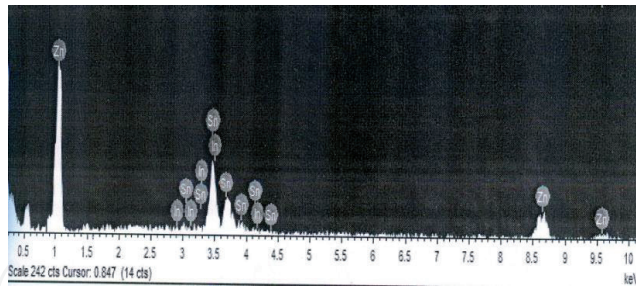


Figure 6.
Spectrum 3 EDAX graph.

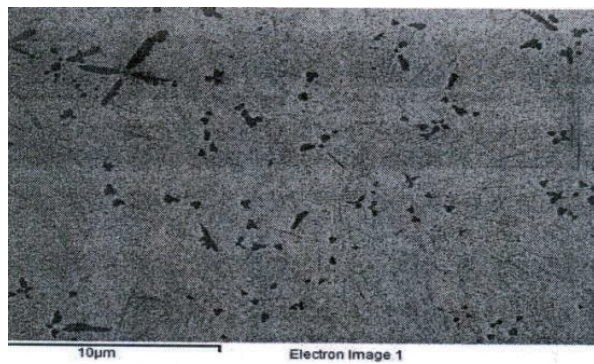


Figure 7.
Spectrum 10 electron image.

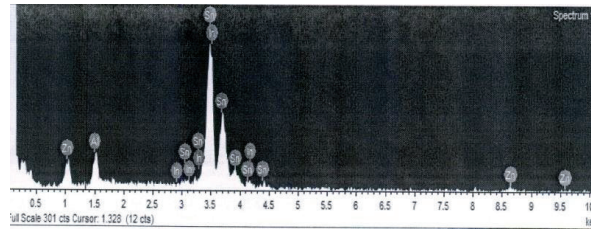


Figure 8.
Spectrum 10 EDAX graph.

It is seen that 1.91% sigma phase is present in the Zn peak, whereas the indium peak, which occurs as two small peaks in the tin cluster, shows 0.20% sigma phase.

Figures 7 and 8 show the microstructure and EDAX at another location. Here, sigma phase is 1.50% in the Zn peak and 0.55% in the aluminium peak. Indium peaks show 0.1% sigma and 1.425 sigma, respectively.

5.2 Analysis of high Al-high indium alloys

Similar results on the microstructure and EDAX analysis of 87Sn–7Zn–3Al–3In and 87.5Sn–6Zn–2Al–2.5 in lead-free soldering alloys are presented below.

5.2.1 Microstructural analysis

Needle shaped Zn phase and leaf shaped Aluminium phase are equally distributed in the microstructure. with the former contributing to increase in strength of the alloy. In the first alloy, the chemical composition of the needle- and leaf-shaped morphologies is given as follows: Leaf-shaped morphology (Al, 88%; Zn, 12%) and needle-shaped morphology (In, 72%; Zn, 27.96%; and Sn, 0.02%). In the second alloy, composition of the leaf- and needle-shaped morphologies is given as follows:



Figure 9.
Examination on leaf shape of the specimen.

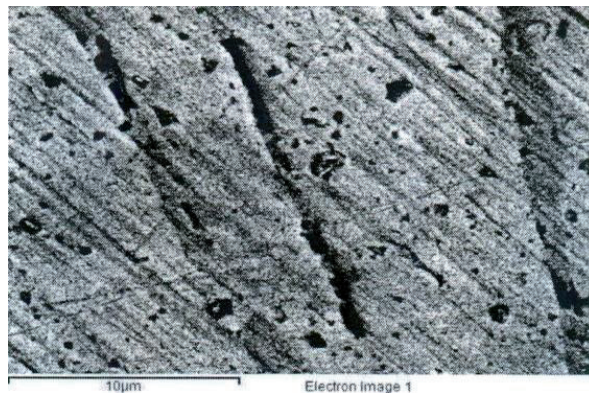


Figure 10.
Examination on needle shape of the specimen.

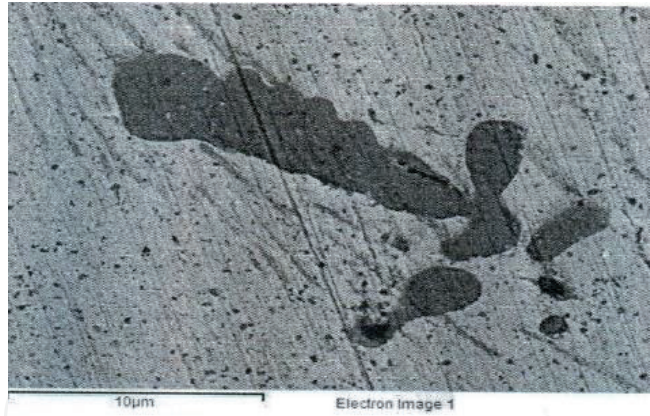


Figure 11.
Examination on leaf shape of the specimen.

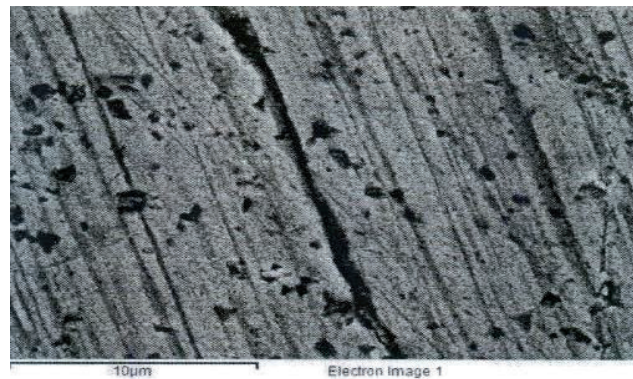


Figure 12.
Examination on needle shape of the specimen.

Leaf-shaped morphology (Al, 91.6%; Zn, 8.4%) and needle-shaped morphology (In, 66.36%; Zn, 31%; and Sn, 2.64%) (**Figures 9–12**).

5.2.2 EDAX analysis

EDAX analysis for both the alloys is presented in **Figures 13–16**. In both cases, the leaf-shaped morphology showed no intermetallics, whereas the needle-shaped morphology showed intermetallics.

Rod-like zinc-rich phases have been observed when cerium and lanthanum of the order of 0.1 wt.% are added [18]. In the current work, since the weight % of rare earth element indium added is relatively high, in all probability, the needle-like phase is rich in indium (72 and 66.36%, respectively) and zinc percentage is lesser,

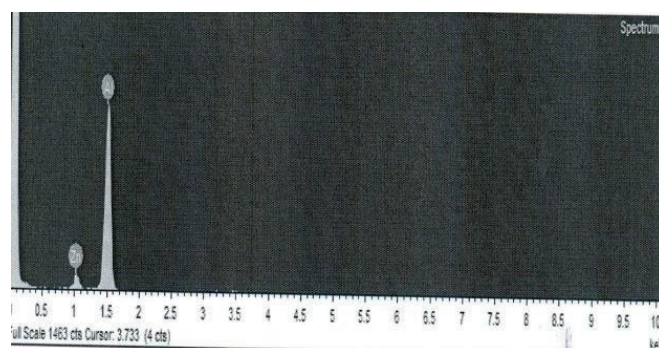


Figure 13.
Chemical composition of the leaf-shaped specimen-alloy 1.

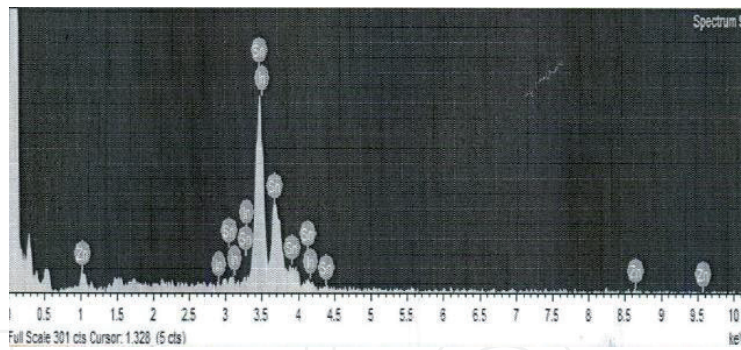


Figure 14.
Chemical composition of the needle-shaped specimen-alloy 1.

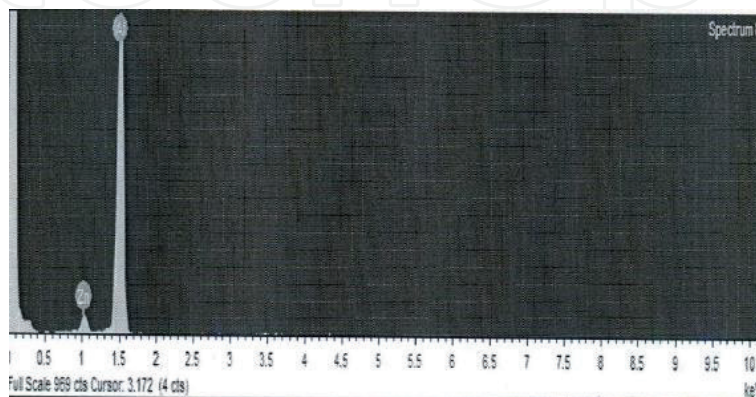


Figure 15.
Chemical composition of the leaf-shaped specimen-alloy 2.

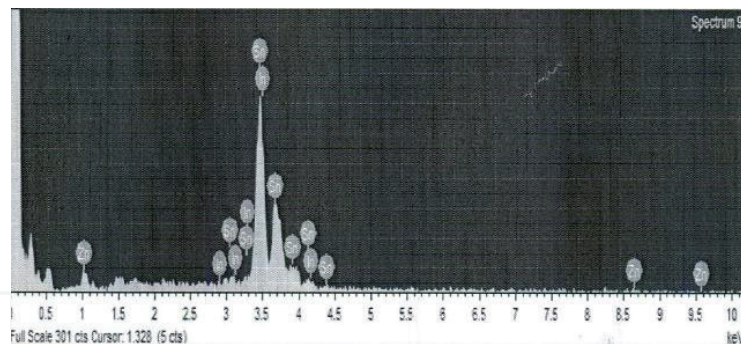


Figure 16.
Chemical composition of the needle-shaped specimen-alloy 2.

agreeing with published literature on cerium and lanthanum addition. Gadolinium addition has been found to refine grains of Mg–5Sn–Zn–Al [19].

In some cases, there have been reports of intermetallic formation suppression as a result of the addition of rare earth metals. A study by Huan Lee et al. showed that addition of praseodymium reduced the formation of intermetallics at the junctions of a Sn–Zn–Ga solder [20].

5.3 Microstructural analysis of Sn–Cu lead-free solders

Figure 17(a, b) shows the dendritic structure of 87Sn–7Cu–3.0Mn–3Ag. The dendrite structure is not seen in the second sample. We can infer that the dendrites are broken down in the second sample. Han et al. [10] and Yang et al. [21] also have reported the influence of Ni-coated carbon addition on the microstructure of Sn3.5Ag0.7Cu nanocomposite solder. It is found that the morphology of Ag₃Sn and Cu₆Sn₅ was

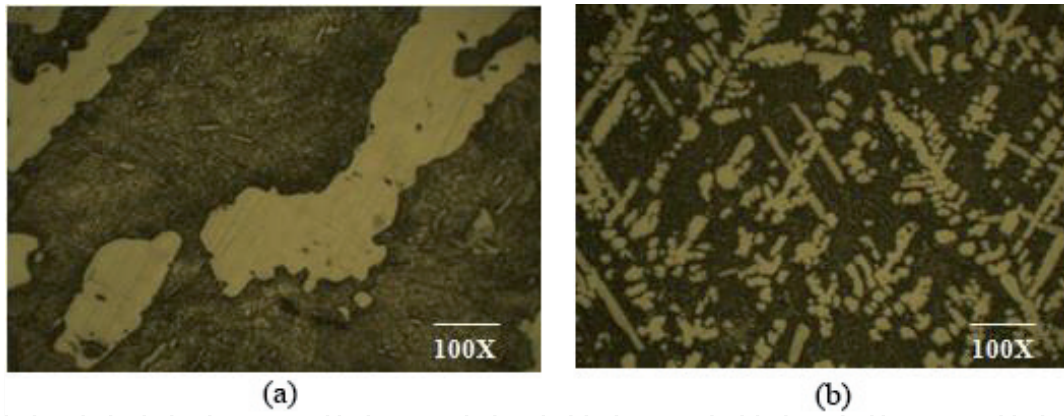


Figure 17. Microstructures of (a) 87Sn—7Cu—3.0 Mn ig. 5. Microstructures of (b) 87.5Sn—7.5Cu—2.5Mn—2.5Ag.

uniformly distributed in the solder matrix. But the addition of another fourth element to form a quaternary changes the microstructure. Some researchers produced intermetallics, which react with Sn, thus refining the microstructure of Sn, Ag and Cu solder. Other researchers chose to add some low solubility and diffusivity in Sn, such as Al_2O_3 , TiO_2 , SiC and POSS. In general, it was found that until a critical value of alloying element content, properties are enhanced, and above this % age, it becomes detrimental to the alloy.

So, addition of Manganese seems to have increased the melting point. The slight difference in melting temperatures could be due to the difference in alloying elements in each sample. Addition of 0.2% iron to SnAg Cu alloys results in two exothermic peaks at 220 and 235°C. When adding 0.6 wt.% Fe, only a single endothermic peak at 221.35°C was found, showing that it has a eutectic composition [22]. Based on the ternary SnAgCu phase diagram [23], there are two steps in the DSC. This could be because of melting of ternary eutectic $\beta\text{-Sn} + \text{Ag}_3\text{Sn} + \eta\text{Cu}_6\text{Sn}_5$ phase and melting of primary $\beta\text{-Sn}$.

6. SEM fractography

SEM micrographs are generally used to give information about the type of fracture. Here, since tensile tests have not been done, SEM has been used to identify Sn whiskers. There have been some studies showing Sn whiskers in the SEM micrographs of SnCu alloys.

The abovementioned SEM micrographs are of two samples of slightly varying chemical composition. **Figures 18** and **19** show the absence of tin whiskers in both

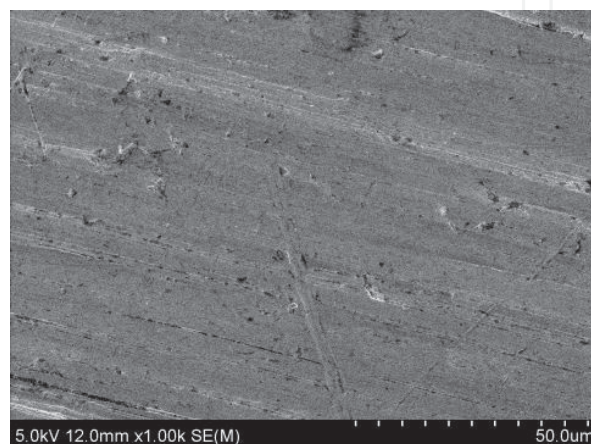


Figure 18.
Sample 1.

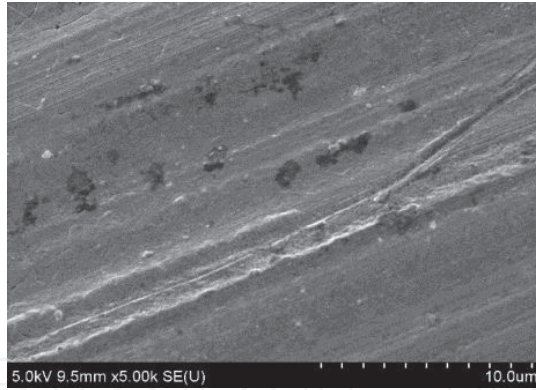


Figure 19.
Sample 2.

the alloys. The presence of tin whiskers results in deterioration of electrical properties. Chuang and Lin [24] showed that 0.5% Zn addition into SnAgCu solder refined the microstructure and suppressed whisker growth.

Sn—Zn alloys have been used as a substitute for Pb—Sn alloys. However, Sn—Zn alloys are susceptible to oxidation and ZnO forms easily (**Figures 20 and 21**) [25–27].

SEM micrographs are for two different compositions of Sn—Zn—La lead-free solders (composition as mentioned in the Hardness **Tables 4 and 5**). Some

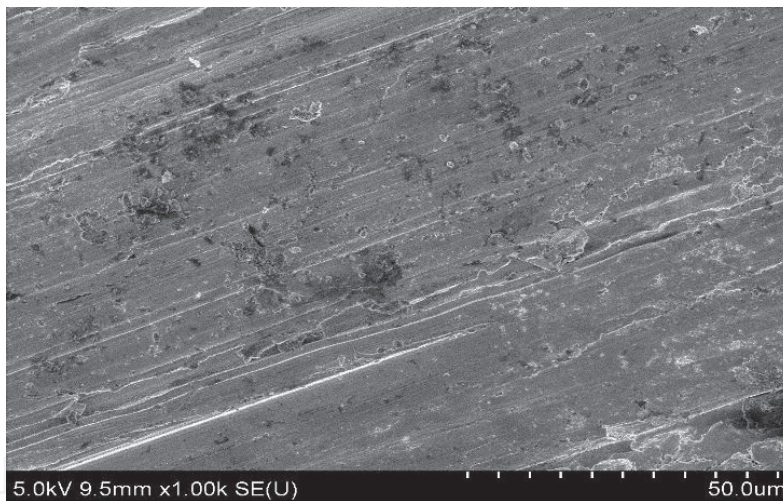


Figure 20.
SEM micrographs of Sn—Zn—La alloys.

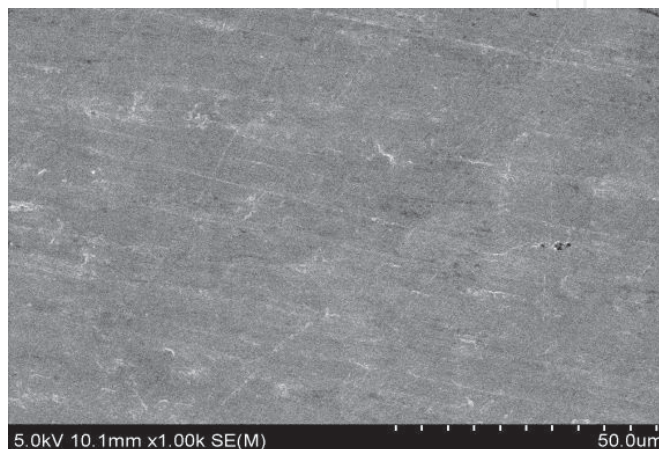


Figure 21.
SEM micrographs of Sn—Zn—La alloys.

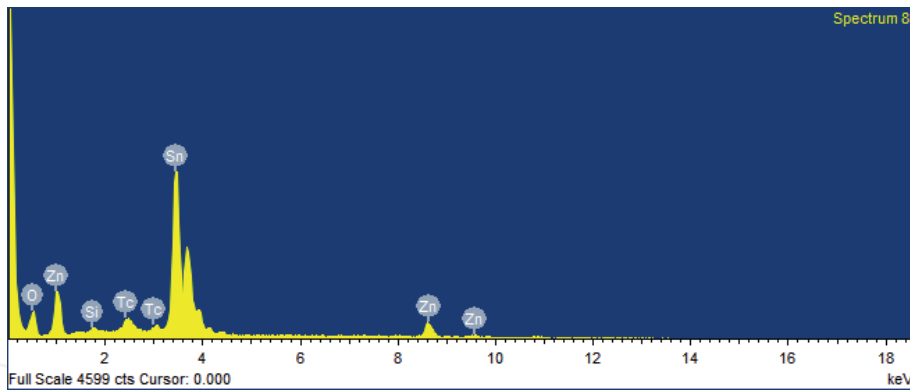


Figure 22.
EDAX of Sn—Zn—La sample.

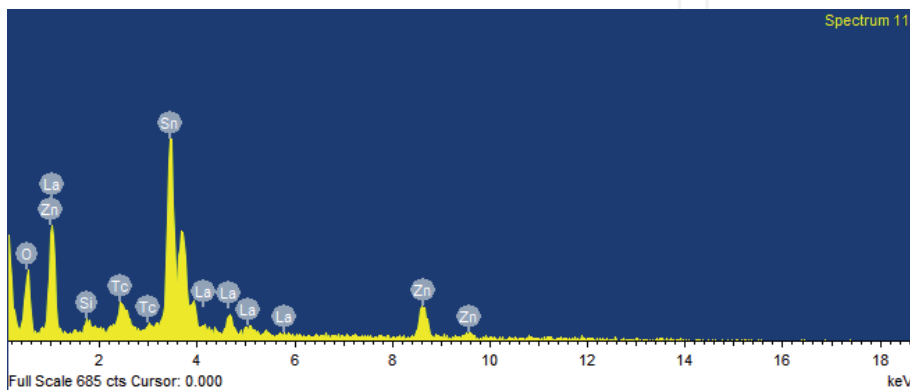


Figure 23.
EDAX of Sn—Zn—La of slightly different composition.

precipitates are seen, which may have an effect on the hardness and tensile strength of the solders. However, in this case, it was found that hardness for both alloys is around 18 H_v. Hence, the effect of precipitates seems to be marginal for this lead-free alloy. These SEM micrographs have been taken from unpublished work done by the author as part of undergraduate project work.

EDAX Studies.

EDAX Studies of two samples (**Figures 22 and 23**).

There is not much difference between the EDAX of the two samples. There do not seem to be intermetallics present in this alloy. Hardness values also corroborate this statement.

7. Conclusion

This chapter starts with the importance of intermetallic systems in lead-free solders. The effect of some rare earths like lanthanum and indium on intermetallic formation in lead-free alloys has been explained. Tin-zinc-lanthanum and tin-zinc-aluminium-indium have been chosen for detailed analysis. Microhardness surveys have been done along two perpendicular diagonals of a square-shaped specimen, and the results of the microhardness surveys have been analysed. Microstructures in both these systems have been discussed with respect to the phases present and their distribution. Based upon both the microhardness and microstructure of the two alloys chosen, the presence of intermetallics and the types of intermetallics has been discussed. Growth kinetics of intermetallics has been briefly analysed. SEM fractographs have been taken to show the type of fracture. EDAX has been employed to show the distribution of phases.

IntechOpen

Author details

Dattaguru Ananthapadmanaban^{1*} and Arun Vasantha Geethan²

1 Department of Mechanical Engineering, SSN College of Engineering,
Chennai, India

2 Department of Mechanical Engineering, St. Josephs Institute of Technology,
Chennai, India

*Address all correspondence to: ananthapadmanaban.dattaguru@gmail.com

IntechOpen

© 2019 The Author(s). Licensee IntechOpen. This chapter is distributed under the terms of the Creative Commons Attribution License (<http://creativecommons.org/licenses/by/3.0>), which permits unrestricted use, distribution, and reproduction in any medium, provided the original work is properly cited. 

References

- [1] Zakraysek L. Intermetallic Growth in Tin-Rich Solders, *Welding Research Supplement*; 1972. pp. 536-541
- [2] Faizal SM, Azlina OS. Intermetallic compound formation on lead-free solders by using microwave energy. *AIP Conference Proceedings*. 2016;**1774**:060008
- [3] Roubaud P, Ng G, Bulwith GH-HPR, Prasad RH-AMS, Kamath FC-CPACS, Garcia-Sanmina A. Impact of intermetallic growth on the mechanical strength of Pb-free BGA assemblies. In: *APEX 2001 International Conference*. San Diego; 2001
- [4] Wassink R, Klein J. *Soldering in Electronics*. 2nd ed. Ayr, Scotland: Electrochemical Publications Limited; 1989
- [5] Li GY, Chen BL. Formation and growth kinetics of interfacial intermetallics in Pb-free solder joint. *IEEE Transactions on Components and Packaging Technologies*. 2003;**26**(3):651-658
- [6] Zhao N, Zhong Y, Huang ML, Ma HT, Dong W. Growth kinetics of Cu_6Sn_5 intermetallic compound at liquid-solid interfaces in Cu/Sn/Cu interconnects under temperature gradient. *Scientific Reports*. 2015;**5**:13491
- [7] Guo MY, Lin CK, Chen C, Tu KN. Asymmetrical growth of Cu_6Sn_5 intermetallic compounds due to rapid thermomigration of Cu in molten SnAg solder joints. *Intermetallics*. 2012;**29**:155-158
- [8] Qu L, Zhao N, Ma HT, Zhao HJ, Huang ML. In situ study on the effect of thermomigration on intermetallic compounds growth in liquid-solid interfacial reaction. *Journal of Applied Physics*. 2014;**115**:204907
- [9] Arthur Jebastine Sunderraj D, Ananthapadmanaban D, Arun Vasantha Geethan K. Chapter 30: Comparative hardness studies and microstructural characterization of 87 Sn-7Zn-3Al-3In and 87.5 Sn-6 Zn-2Al-2.5 in lead free soldering alloys. In: *Advances in Materials and Metallurgy Lecture Series in Mechanical Engineering*. Springer Nature. pp. 311-323
- [10] Arthur Jebastine Sunderraj D, Ananthapadmanaban D, Arun Vasantha Geethan K. Preparation, hardness studies and characterization of 88 Sn-7.5Zn-2.5Al-2In and 88 Sn-7 Zn-2Al-2.5 in lead free soldering alloys. In: *IOP Conference Series, Materials Science and Engineering*. 2018
- [11] Steward T, Liu S. *Database for Solder Properties with Emphasis on New Lead Free Solders*. National Institute for Standards and Technology and Colorado School of Mines; 2002
- [12] Budi Dharma IGB, Hamdi M, Ariga T. The effects of adding silver and indium to lead-free solders. *Welding Journal*. 2009;**88**(4):45-47
- [13] Shalaby RM. Effect of indium content and rapid solidification on microhardness and micro-creep of Sn-Zn eutectic lead free solder alloy. *Crystal Research and Technology*. 2010;**45**(4):427-432
- [14] Wang Y-T, Ho CJ, Tsai H-L. Effect of in addition on mechanical properties of Sn-9Zn-In/Cu solder. In: *8th IEEE International Conference on Nano/Micro Engineered and Molecular Systems. Nano/Micro Engineered and Molecular Systems (NEMS)*; 2013
- [15] Aamir M, Muhammed R, Ahmed N. Mechanical properties of lead free solder alloy for green electronics under high strain rate and thermal aging. *Journal of Engineering and Applied Science*. 2017;**36**(1):115-123

- [16] Zhang L, Fan XY, Guo YH, He CW. Properties enhancement of SnAgCu solders containing rare earth Yb. *Materials and Design*. 2014;**57**:646-651
- [17] Tay SL, Haseeb ASMA, Johan MR, Munroe PR, Quadir MZ. Influence of Ni nanoparticle on the morphology and growth of interfacial intermetallic compounds between Sn-3.8Ag-0.7Cu lead-free solder and copper substrate. *Intermetallics*. 2013;**33**:8-15
- [18] Wu CML, Law CMT, Yu DQ, Wang L. The wettability and microstructure of Sn-Zn-RE alloys. *Journal of Electronic Materials*. 2003;**32**(2):63-69
- [19] Fang CF, Meng LG, Wu YF, Wang LH, Zhang XG. Effect of Gd on the microstructure and mechanical properties of Mg-Sn-Zn-Al alloy. *Applied Mechanics and Materials*. 2013;**312**:411-414
- [20] Ye H, Xue S, Luo J, Lee Y. Properties and interfacial microstructure of Sn-Zn-Ga solder joint with rare earth Pr addition. *Materials and Design*. 2013;**46**:316-322
- [21] Yang ZB, Zhou W, Wu P. Effects of Ni-coated carbon nanotubes addition on the microstructure and mechanical properties of Sn-Ag-Cu solder alloys. *Materials Science and Engineering A*. 2014;**590**:295-300
- [22] El-Daly AA, Hammad AE, Al-Ganainy GS, Ragab M. Influence of Zn addition on the microstructure, melt properties and creep behavior of low Ag-content Sn-Ag-Cu lead free solders. *Materials Science and Engineering A*. 2014;**608**:130-138
- [23] Shnawah DA, Sabri MFM, Badruddin IA. A review on thermal cycling and drop impact reliability of SAC solder joint in portable electronic products. *Microelectronics Reliability*;52(1):90-99
- [24] Chuangand TH, Lin HJ. Inhibition of whisker growth on the surface of Sn-3Ag-0.5Cu 0.5Ce solder alloyed with Zn. *Journal of Electronic Materials*. 2009;**38**(3):420-424
- [25] Hirose A, Yanagawa H, Ide E, Kobayashi KF. Joint strength and interfacial microstructure between Sn-Ag-Cu and Sn-Zn-Bi solders and Cu substrate. *Science and Technology of Advanced Materials*. 2004;**5**:267
- [26] Iwasaki T, Kim JH, Mizuhashi S, Satoh M. Encapsulation of lead-free Sn/Zn/Bi solder alloy particles by coating with wax powder for improving oxidation resistance. *Journal of Electronic Materials*. 2005;**34**:647
- [27] McCormack M, Jin S, Chen HS. Wetting interaction of Pb-free Sn-Zn-Al solders on metal plated substrate. *Journal of Electronic Materials*. 1994;**23**:687